RSC Advances

ROYAL SOCIETY OF CHEMISTRY

www.rsc.org/advances

Journal Name

ARTICLE

C-8 Mannich base derivatives of baicalein display improved glucuronidation stability: exploring the mechanism by experimentation and theoretical calculations

Received 00th January 20xx,
Accepted 00th January 20xx

DOI: 10.1039/x0xx00000x

www.rsc.org/

Guiyuan He[a,b], Shixuan Zhang[c], Liang Xu[d], Yangliu Xia[a,b], Ping Wang[a], Shiyang Li[a], Liangliang Zhu[a], Hongxi Xu[e], Guangbo Ge*[a,c],Ling Yang*[a]

Baicalein(BA), a natural flavonoid compound, possesses many desirable pharmacological activities. However, poor solubility and extensive metabolism by human UDP-glucuronosyltransferases (UGTs) strongly restrict the clinical applications of BA. We previously reported that two C-8 Mannich base derivatives of BA (BA-a and BA-j) displayed enhanced solubility and anti-cyclin dependent kinase 1 activity, yet the metabolic stabilities of these compounds remained unknown. This study aimed to evaluate the *in vitro* glucuronidation stability of these BA derivatives and to explore the key factors affecting the UGT-mediated biotransformation. The results showed that the glucuronidation stabilities of these BA derivatives were much higher than BA. BA-a exhibited 12-fold and BA-j exhibited 5-fold improved stability in human liver S9, while in human intestine S9, BA-a and BA-j exhibited 42 –fold and 33-fold improved stability, respectively. Further investigations found that the major glucuronidation site(s) were changed from 7-OH and 6-OH in BA to 6-OH in the BA derivatives. Also, both the involved enzymes and their catalytic efficacy in 6-O-glucuronidation of BA derivatives were much lower than that of BA. The formation of an intramolecular hydrogen bond between the C-8 Mannich base substituents and C-7 phenolic groups played a predominant role in these glucuronidation changes. The calculated bond dissociation energy (BDE) of each phenolic group in BA and its derivatives agreed well with their glucuronidation activities. All these findings bring new insights into the structure-glucuronidation relationship and provide a practical strategy for the structural modification to improve the glucuronidation stability of drug candidates, especially for those phenolic compounds.

Introduction

Baicalein (BA), a flavonoid compound, was originally isolated from the Chinese herb *Scutellariabaicalensis* (Huang-Qin). In the past twenty years, pharmacological studies have demonstrated that BA possesses many desirable bioactivities including anti-cancer,[1-3] anti-inflammatory,[4,5] anti-oxidation,[6,7] and anti-viral activity.[8,9] However, poor solubility and rapid metabolic clearance by phase II drug metabolizing enzymes are the major barriers for its *in vivo* pharmacological activities. BA is almost insoluble in water but soluble in organic solvents such as DMSO and methanol. BA contains three phenolic hydroxyls (5-OH, 6-OH and 7-OH) (Fig. 1) and these are the preferred metabolic sites for phase II drug metabolizing enzymes. Previous studies demonstrated that 7-O- and 6-O-glucuronidation were the predominant human metabolic pathways of BA, while sulfation and methylation also occurred but to a lesser extent.[10-13] Human UDP-glucuronosyltransferases (UGTs) including UGT1A1, UGT1A3, UGT1A8, UGT1A9 and UGT2B15 were reported to catalyze the O-glucuronidations of BA.[11] UGT is the most important phase II drug-metabolizing enzyme in human which is expressed in many organs, and responsible for the metabolic elimination of 10% of the top 200 prescribed drugs in the USA.[14] Extensive first-pass metabolism by human intestinal and hepatic UGTs

[a] Laboratory of Pharmaceutical Resource Discovery, Dalian Institute of Chemical Physics, Chinese Academy of Sciences, Dalian, China.
E-mail: geguangbo@dicp.ac.cn; yling@dicp.ac.cn
Tel: 0086-8437-9317Fax: 0086-41184676961
[b] University of Chinese Academy of Sciences, Beijing 100049, China.
[c] State Key Laboratory of Fine Chemicals, Dalian University of Technology, Dalian 116012, China.
[d] College of Chemistry, Dalian University of Technology, Dalian, 116024, China
[e] Shanghai University of Traditional Chinese Medicines, Shanghai, 201203, China.
†Electronic Supplementary Information (ESI) available: The 1H NMR, 13C NMR, HSQC and HMBC spectra for BA-a, BA-a 6-O-glucuronide, BA-j and BA-j 6-O-glucuronide. See DOI:10.1039/x0xx00000x

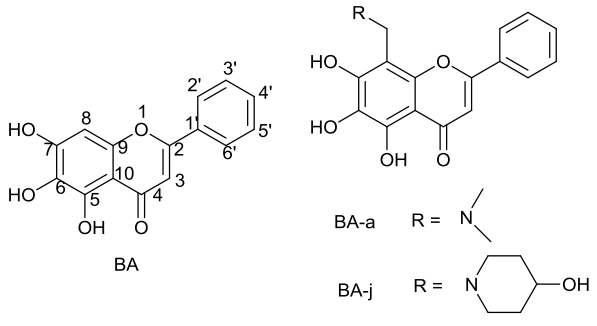

Fig. 1 Chemical structures of baicalein and its C-8 derivatives

has been recognized as one of the major reasons for the low bioavailability of BA.[11] Like BA, many other natural flavonoids are preferred substrates of human UGTs, multiple UGT isoforms display rapid glucuronidation ability for these phenolic compounds.[15-17] The rapid metabolic clearance by human UGTs is one of the main reasons for the poor bioavailability and short half-life of natural flavonoids in human.[18] Therefore, novel flavonoids with both high bioactivity and improved metabolic stability are much in demand. In the past twenty years, many structural modifications of BA have been made and have generated a variety of structurally diverse derivatives of BA. However, to the best of our knowledge, most of the studies focused on improving bioactivities,[19,20] the evaluation of metabolic stabilities of BA derivatives was rarely reported.

UGT-mediated O-glucuronidation of flavonoids demonstrated strong region-selective features, in which the phenolic group at C-5 was hardly glucuronidated.[15] The high glucuronidation stability of 5-OH in flavonoids might be attributed to the formation of an intramolecular hydrogen bond (IMHB) between the 5-OH and the carbonyl at the C-4 site.[21-23] Inspired by this, we assumed that introducing a hydrogen bond acceptor at the C-8 site to form an IMHB with 7-OH of BA might block the 7-O-glucuronidation and thus improve the metabolic stability of BA. To verify this, a series of nitrogen-containing derivatives of BA were synthesized via the Mannich reaction and their bioactivities were initially evaluated.[24,25]Among these derivatives, 8-((dimethylamino) methyl)-5,6,7-trihydroxy-flavonoid (BA-a) and 5,6,7-trihydroxy-8-((4-hydroxypiperidin-1-yl) methyl)-flavonoid (BA-j) displayed enhanced solubility and cyclin-dependent kinase 1(CDK1) inhibitory activity.[24,25] Both BA-a and BA-j have a nitrogen-containing substituent at the C-8 position in which the amine could interact with the C-7 phenolic group and form an IMHB (Fig. 1). Although this structural modification improved the bioactivity and solubility, the metabolic stability (especially the UGT mediated glucuronidation stability) of these BA derivatives remained unknown. The aim of this study was to evaluate the *in vitro* glucuronidation stability of these BA derivatives and to explore the key factors affecting the UGT mediated biotransformation.

In this study, the *in vitro* UGT-mediated metabolism of BA-a and BA-j were systematically investigated and BA was used as a reference compound. A series of *in vitro* assays including the glucuronidation half-life, the glucuronidation profile, the screening of recombinant human UGTs and the kinetic analysis of the major UGTs involved and HLM were carried out. Furthermore, the bond dissociation energy (BDE) of hydroxyls in BA, BA-a and BA-j were calculated to help interpret the preferred metabolic site(s) of these flavonoids.

Results

In vitro Half-life Assays

To evaluate the glucuronidation stability, *in vitro* half-life assays for three compounds (BA, BA-a and BA-j) were carried out in both human liver S9 (HLS9) and human intestine S9 (HIS9) under physiological conditions (pH 7.4 at 37 °C), in the presence of UDP-glucuronic acid (UDPGA). The results demonstrated that the glucuronidation stability of BA derivatives were much higher than that of BA in both tissues. In HLS9, BA-a displayed 12-fold and BA-j exhibited 5-fold improved glucuronidation stability. In HIS9, BA-a exhibited 42-fold and BA-j exhibited 33-fold greater stability with respect to BA (Table 1).

Table 1 BA, BA-a and BA-j UGT metabolism half-life in HLS9 and HIS9.

Enzyme source	$t_{1/2}$(min)		
	BA	**BA-a**	**BA-j**
HLS9	25.02±7.22	290.31±27.04	123.00±4.6
HIS9	9.80±1.34	417.89±14.11	329.18±59.73

Glucuronidation Profiles and Metabolites Characterization

To further investigate the impact of such structural modifications on the UGT-mediated metabolism of BA derivatives, the metabolic profiles of BA, BA-a and BA-j in HLM and human intestine microsomes (HIM) were investigated and the major metabolites were biosynthesized and characterized by NMR spectra.

Two glucuronides of BA could be easily detected in both HLM and HIM following 10 min incubation, in the presence of UDPGA (Fig. S1, ESI†), which agreed well with the previous studies on BA-O-glucuronidation conducted in HLM or RLM.[11-13] In both HLM and HIM, a single metabolite could be detected in BA-j following 1 hour incubation, in the presence of UDPGA. For BA-a, one metabolite could be clearly detected in both HLM and HIM following 1 hour incubation under the same conditions. The amount of the glucuronide in HLM was higher than that in HIM. The metabolites of BA, BA-a and BA-j showed a molecular ion $[M-H]^-$ at *m/z* 445, *m/z* 502, and *m/z* 558 respectively in negative-ion mode, which increasing *m/z* 176 compared with the molecular ion $[M-H]^-$ of the corresponding substrate. Thus, these metabolites were identified as mono-glucuronides. The mass spectra of BA, BA-a and BA-j and their corresponding mono-glucuronides are provided in the supporting materials (Fig. S2, ESI†). In Fig. 2, the amount of the mono-glucuronide of both BA-a and BA-j in HLM was higher than that in HIM, which was consistent with the results from *in vitro* half-lives. The major glucuronidation site(s) of BA and its two derivatives were also identified. Two BA glucuronides in HLM and HIM were identified as 7-O-glucuronides and 6-O-

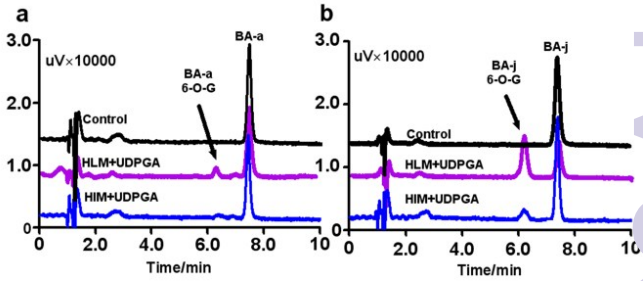

Fig. 2 Glucuronidation metabolic profiles of BA-a (a) and BA-j (b) in HLM and HIM. BA-a or BA-j (10 μM) was incubated with HLM or HIM in the presence of UDPGA for 60 min.

Journal Name

ARTICLE

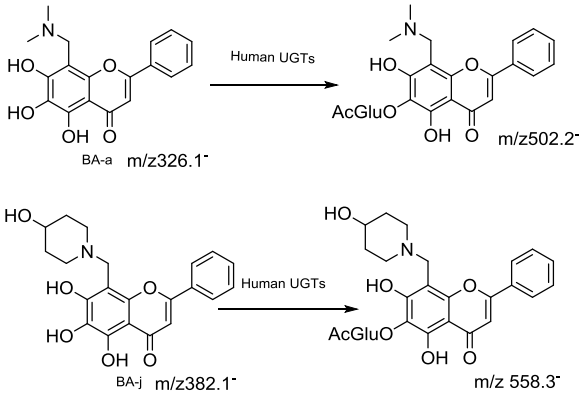

Fig. 3 Glucuronidation of BA-a and BA-j in HLM

glucuronides, respectively, based on the LC retention times, UV and MS spectra of standards. The major glucuronides of BA-a and BA-j were biosynthesized using rabbit liver microsomes (RbLM) as the enzyme source. Their chemical structures were fully characterized as 6-O-glucuronides using ^{1}H-NMR, ^{13}C-NMR, and HSQC and HMBC NMR techniques (Fig. S5-16, ESI†). The chemical shift of ^{1}H-NMR, ^{13}C-NMR of BA-a, BA-a 6-O-glucuronide, BA-j and BA-j 6-O-glucuronide are provided in Table S1-2(ESI†). A correlation between G1-CH (4.52-4.53 ppm) and C-6 (131.33 ppm) in HMBC spectra of BA-a glucuronide was detected, which could assigned the metabolite as 6-O-glucuronide of BA-a. In HMBC spectra of BA-j-G, correlation between G1-CH (4.56 ppm) and C-6 (131.20 ppm) was found, thus the glucuronide of BA-j in HLM was identified as 6-O-glucuronide as well (Fig. S4, ESI†). The coupling constants (J) for the anomeric proton of these two 6-O-glucuronides (the glucuronic acid moiety) are large than 7.0 Hz, suggesting that these two 6-O-glucuronides are β-glucuronide.[26] In addition, hydrolysis of these metabolites by β-glucuronidase also confirmed that these glucuronides are β-glucuronides. All these findings suggested that BA could be glucuronidated at both 7-OH and 6-OH, but BA-a and BA-j displayed strong region-selectivity O-glucuronidation at 6-OH.

Assignment of Involved Human UGTs

To compare the human UGT isoforms involved in O-glucuronidation of BA, BA-a and BA-j, a panel of 12 recombinant human UGT isoforms (UGT1A1, 1A3, 1A4, 1A6, 1A7, 1A8, 1A9, 1A10, 2B4, 2B7, 2B15, and 2B17) were tested for their ability to glucuronidate these compounds (Fig 4). Of the screened 12 recombinant UGT isoforms, 9 (UGT1A1, 1A3, 1A6, 1A8, 1A9, 1A10, 2B7, 2B15 and 2B17) were involved in BA-O-glucuronidations. In contrast, only 6 isoforms were involved in BA-a O-glucuronidation or BA-j O-glucuronidation. The isoforms involved in BA-a and BA-j glucuronidation were the same, including UGT1A1, 1A3, 1A8, 1A9, 2B15 and 2B17. Among the involved enzymes, UGT1A9 displayed the highest efficiency in BA-a 6-O-glucuronidation, while UGT1A1 showed the highest efficiency in BA-j 6-O-glucuronidation. Other UGT isoforms, including UGT1A6, UGT1A10 and UGT2B7 did not show evidence of catalytic activities in BA-a or BA-j glucuronidation whereas they were significantly active to glucuronidate BA.

Kinetic Analysis

In order to compare the intrinsic clearances of these two derivatives with BA, kinetic analysis of BA, BA-a, and BA-j O-glucuronidation were performed in HLM, UGT1A1 and UGT1A9. The formation of O-glucuronides of BA and its derivatives followed either Michaelis-Menten kinetics or substrate inhibition kinetics (Table 2&Fig 5). In HLM, the intrinsic clearances of BA were 78-fold higher than that of BA-j and 251-fold higher than that of 6-O-glucuronide formation of BA-a. The decreased intrinsic clearances of BA derivatives were

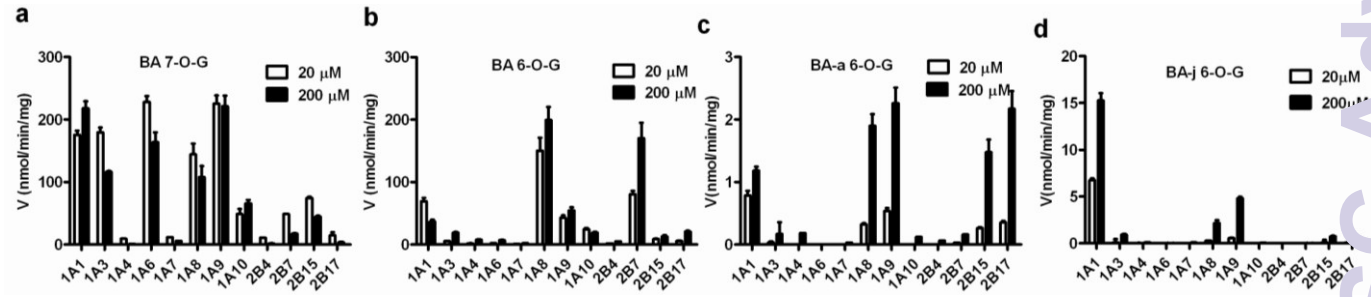

Fig. 4 Reaction phenotyping of BA (a, b), BA-a (c) and BA-j (d) with a panel of human recombinant UGTs. The final substrate concentrations were 20 μM a 200 μM, respectively. All samples were incubated under physiological conditions (pH 7.4 at 37 °C) for 60 min, in the presence of UDPGA.

Journal Name

ARTICLE

Table 2 Kinetic parameters of BA, BA-a and BA-j O-glucuronidations in HLM and selected human recombinant UGTs.

Compound	Enzyme sources	K_m μM	V_{max} nmol/min/mg	K_{si} μM	V_{max}/K_m nmol/min/mg	Kinetic model
BA (7-O-G)	HLM	51.23	54.05		1055.12	Michaelis-Menten
BA (6-O-G)	HLM	63.18	5.81	1906.86	91.98	Substrate inhibition
BA-a (6-O-G)	HLM	198.18	0.90		4.56	Michaelis-Menten
	UGT1A1	66.44	0.17		2.52	Michaelis-Menten
	UGT1A9	107.8	0.33	805.8	3.05	Substrate inhibition
BA-j (6-O-G)	HLM	285.3	4.17	618.3 7	14.61	Substrate inhibition
	UGT1A1	69.77	4.26	1372.19	61.03	Substrate inhibition
	UGT1A9	204.05	1.15	569.42	5.62	Substrate inhibition

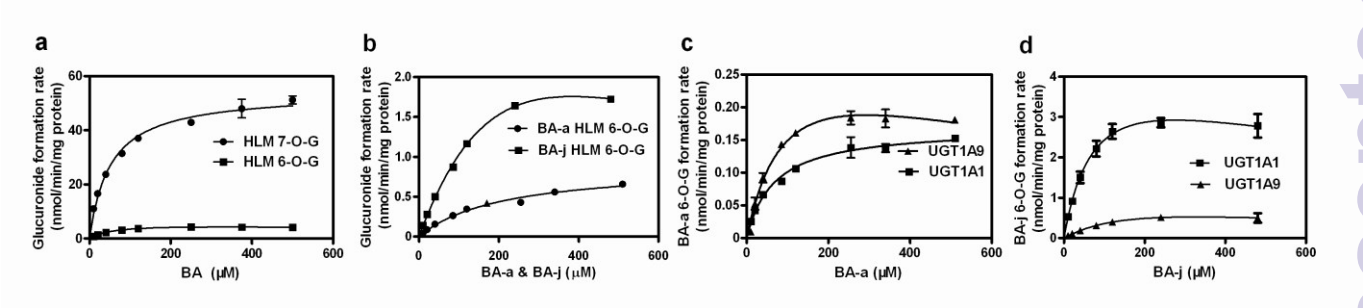

Fig. 5 Kinetic analysis. (a) BA-O-glucuronidations in HLM; (b) BA-a and BA-j 6-O-glucuronidations in HLM; (c) BA-a 6-O-glucuronidation in UGT1A1 and UGT1A9; (d) BA-j 6-O-glucuronidation in UGT1A1 and UGT1A9.

caused by both the increase of K_m values and the decrease of the V_{max} values. In HLM, the K_m values for 6-O-glucuronidation and 7-O-glucuronidation of BA were 63 μM and 51 μM respectively, which were much lower than that of 6-O-glucuronidation of BA-a (198 μM) and BA-j (285 μM).The V_{max} values of BA 6-O-glucuronidation and 7-O-glucuronidation were 6 times and 54 times greater than that of 6-O-glucuronidation of BA-a in HLM. The V_{max} value of BA 6-O-glucuronidation was slightly higher than that of 6-O-glucurondation of BA-j, but the V_{max} value of 7-O-glucurondation of BA was 14 times higher than that of 6-O-glucurondation of BA-j in HLM. The same trend was also observed with the kinetic analysis in recombinant human UGTs. The reported K_m values of BA 7-O-glucuronidation in recombinant human UGTs ranged from a few micromolar to 20 μM,[11] which were much lower than that of the K_m values of BA-a and BA-j 6-O-glucuronidation in UGT1A1 and UGT1A9 (60-200 μM). The intrinsic clearance for BA 7-O-glucuronidation in UGT1A1 and UGT1A9 were about 330 nmol/min/mg and 640 nmol/min/mg respectively,[11] which were much greater than that of 6-O-glucurondation of BA-a and BA-j in UGT1A1 and UGT1A9 (2-60 nmol/min/mg).

Calculation of Bond Dissociation Energy

In order to further explain the region-selective glucuronidation of BA derivatives from the view of reaction energy, the bond dissociation energy (BDE) or hydrogen dissociation energy of all phenolic groups in BA, BA- a and BA-j were calculated theoretically for the first time. As shown in Table 3, of the three phenolic groups in BA, the BDE of 5-OH is the highest (80.2 kcal/mol), while BDEs of 6-OH and 7-OH are considerably low, implying that the glucuronidation of 6-OH and 7-OH are easy while the glucuronidation of 5-OH is difficult. The BDEs calculations are highly consistent with the experimental results. The same consistency was also demonstrated between the experimental results and the calculations of BA derivatives.

Table 3 Calculated BDEs of each phenolic group in BA, BA-a and BA-j.

Hydroxyls	BDE (kcal/mol)		
	BA	BA-a	BA-j
5-OH	80.20	85.33	85.45
6-OH	64.07	77.28	77.33
7-OH	65.20	86.30	85.67

The BDEs of all phenolic groups of BA-a and BA-j followed the same order, which is 7-OH>5-OH>6-OH. From the view of the activation energy barrier, 6-OH is the most possible metabolic site for O-glucuronidation of BA-a and BA-j, while the glucuronidations at 7-OH and 5-OH were required higher energy and were thus not glycosylated. The experimental results indicated that 6-OH was the preferred glucuronidation site(s) of BA-a and BA-j. Furthermore, it is evident from Table 3 that the BDEs of 6-OH and 7-OH of BA are much lower than that of the corresponding hydroxyls in BA-a and BA-j, which was consistent with the experimental results in which both BA 6-O and 7-O glucuronidations displayed much higher velocity and efficiency than 6-O glucuronidation of BA-a and BA-j. All these findings strongly suggested that the BDE of phenolic group is one of the key factors affecting the region-selective glucuronidation of BA and its derivatives. As hydrogen dissociation is the prerequisite for O-glucuronidation (a typical SN2-reaction) and this step needs to overcome an energy barrier.

Discussion

Structural modification is a widely used strategy for improving the metabolic stability of lead compounds or drug candidates in drug discovery. Previously, dimethylamino-methyl substitutes have been used in the structural modifications from SN-38 (7-ethyl-10-hydroxycamptothecin) to topotecan and the synthesis of C-8 Mannich base derivatives of esculetin.[42-44] These modifications shared the same features where the dimethylamino-methyl group can form an IMHB with its adjacent phenolic group. Both modifications showed improved glucuronidation stability, yet the underlying mechanism remained unknown. By comparing the *in vitro* UGT metabolism of BA and its two derivatives, this study used experimental methods and theoretical calculations to reveal for the first time that the mechanism of IMHB formed at the major glucuronidation site could enhance the glucuronidation stability. Key factors which affect the UGT-mediated biotransformation are also discussed.

Our experimental results demonstrated that there are three major differences between the glucuronidation of BA and its two derivatives. First, the metabolic sites were different. For BA, both the 6-OH and 7-OH could be easily glucuronidated by human UGTs, but for BA-a and BA-j, the 6-OH was the major glucuronidation site. Second, the UGT isoforms involved in BA-a and BA-j O-glucuronidation were different compared with BA O-glucuronidation. Of the 12 isoforms tested, 9 displayed high activities in BA-7-O and 6-O-glucuronidation. However, the UGT isoforms involved in BA-a and BA-j 6-O-glucuronidation were decreased to 6. UGT1A6, 1A10 and 2B7 did not show evidence of catalytic activity in BA-a or BA-j glucuronidation. Third, the catalytic efficacy of BA-a and BA-j O-glucuronidation were decreased significantly compared with BA O-glucuronidation. The intrinsic clearances of BA O-glucuronidation were 78 times higher than that of BA-j and 251 times higher than that of 6-O-glucuronidation of BA-a in HLM. The reduced intrinsic clearance was contributed by both the decrease of the V_{max} values and the increase of the K_m values in BA derivatives glucuronidation. Taken together, the glucuronidation stability of BA-a and BA-j were greatly improved by the structural modification.

In HLM, the major metabolic sites of BA were the 7-OH and 6-OH, while the major metabolic site in BA-a and BA-j was the 6-OH. The formation of an IMHB between the 7-OH and the amine of the C-8 substituent of BA-a and BA-j played an important role in this metabolic alteration. Human UGTs belong to the GT1 family; [27] the UGT-mediated reaction is a bi-substrate reaction and follows the SN2-reaction mechanism.[28] Miley et al. suggested that human UGT, like many GT1 enzymes, utilizes a serine protease-like catalytic mechanism in which histidine 35 (of UGT2B7) and aspartate 151 (UGT2B7) function as a catalytic dyad. His 35 attracts the proton of the phenolic group in the acceptor ligand to assist a nucleophilic attack to the anomeric carbon of the glucuronic acid of UDPGA.[29] When the IMHB is formed between the 7-OH and the C-8 substituent of BA-a or BA-j, the attraction of the proton at the 7-OH by histidine 35 of UGT becomes difficult. This was proved by the calculation result that the BDE of the 7-OH of BA-a (86.30 kcal/mol) and BA-j (85.67 kcal/mol) were significantly increased compared with the BDE of the 7-OH of BA (65.20 kcal/mol). Therefore, the IMHB formed at a UGT metabolic site can protect the hydroxyl from being glucuronidated. As the bond energy of the IMHB is not fixed, some weak hydrogen bonds still can be broken and the glucuronidation reaction can proceed. However, the production of the metabolite will be greatly reduced. Some strong hydrogen bonds cannot be broken, thus the glucuronidation reaction is terminated. When the IMHB is formed with BA-a or BA-j, the C-8 substituent no longer rotates freely and becomes fixed facing the 7-OH. This configuration can cause steric hindrance for 7-OH access to the catalytic site of the UGT enzyme. The steric hindrance of the Mannich base substituent can be another reason for the block of the glucuronidation of the 7-OH of BA-a and BA-j.

As the result of structural modification, the involved UGT isoforms for BA-a and BA-j glucuronidation were decreased. UGT1A6, UGT1A10 and UGT2B7 no longer showed evidence of catalytic activity in BA-a or BA-j glucuronidation. UGT1A10 is mainly expressed in intestine and not in liver.[30] UGT2B7 is the most abundant isoform in liver, but also has some expression in intestine.[30] UGT1A6 is expressed in both liver and intestine, while not in a high level.[30] The absence of catalytic activity of UGT1A6, UGT1A10 and UGT2B7 in BA derivative glucuronidation indicated the metabolic stability of the BA derivatives in both human liver and human intestine were improved.

Ethell et al found that increasing the substrate volume results in decreasing the V_{max} for UGT1A6.[31] UGT1A6 prefers to metabolize small planar phenolic and amine compounds;[32] its substrates include coumarins,[33] 1-naphthol, serotonin[34] and protocatechuic aldehyde.[35] We hypothesized that UGT1A6 has a smaller active site than other UGT isoforms and molecular volume can be one of the determinants for its substrate selectivity. In the case of UGT1A10 and UGT2B7, molecular

volume may not be very important for their substrate selectivity. Their substrates include some bulky compounds like steroid. The alteration of other physicochemical properties of substrates such as molecular shape, hydrophobicity or electric charges may be responsible for BA-a and BA-j becoming a poor substrate of UGT1A10 and UGT2B7. Currently, as the crystal structures of the substrate binding area of human UGTs are still unavailable, we cannot further explore the mechanism by molecular docking.

The kinetic analysis displayed a trend that in both HLM and recombinant UGTs, the K_m values of BA derivatives were increased and the V_{max} values of BA derivatives were decreased compared with those of BA. The increased K_m values of BA-a and BA-j indicated that the apparent affinities of these compounds to the enzyme were reduced. Human UGTs are predominantly located in the endoplasmic reticulum and prefer lipophilic compounds as their substrates. The conjugation of a glucuronic acid to a lipophilic substrate leads to increased solubility, thus the substrate can be excreted from the body. Hydrophobic interaction is critical for substrate binding with UGT.[36-39] Xia et al found that esculetin derivatives with a lipophilic substituent at the C-4 position have better affinity for UGT1A9 and UGT1A6 than esculetin.[33] The Mannich base substitutes at the C-8 position decreased the hydrophobicity of these BA derivatives. The cLogP (calculated by ChemBioDraw Ultra13.0) of BA is 3.00, while the cLogPs of BA-a and BA-j are 2.79 and 1.89, respectively. The decreased hydrophobicity might be the main reason for the increased K_m values in BA-a and BA-j kinetics. The decreased V_{max} values in BA-a and BA-j 6-O-glucuronidation are possibly due to the increase in the BDE of the 6-OH. The BDE of the 7-OH and 6-OH of BA are 65.20 and 64.07 kcal/mol respectively, while the BDEs of the 6-OH in BA-a and BA-j are 77.28, and 77.33 kcal/mol, respectively. The BDE calculations strongly suggest that the hydrogen dissociation from the 6-OH of BA-a or BA-j needs to overcome a higher energy barrier, which may explain why the glucuronidation rate of BA-a or BA-j is much lower than that of BA.

Additionally, sulfation and methylation are also human metabolic pathways for BA, besides glucuronidation.[11,13] The reaction mechanisms of sulfation and methylation were also suggested as SN2.[40,41] The structural modification greatly increased the BDEs of the 7-OH and 6-OH of BA-a and BA-j; these hydroxyls were also the metabolic site for sulfation and methylation in BA.[11,13] Therefore, theoretically, the sulfation and methylation reactions of BA-a and BA-j will also be reduced. Our primary result indicated trace amounts of methylation metabolites could be detected but sulfation metabolites were not detected in either BA-a or BA-j HLS9 incubations which contained 3'-phosphoadenosine-5'-phosphosulfate and S-adenosyl methionine cofactors.

In this paper, we first introduced the calculated BDE to help to interpret the UGT metabolic site preference in BA and its derivatives. The experimental results agree well with the calculation of the BDEs, in which the lower BDE has the higher glucuronidation activity. It is interesting that the BDE of both the 7-OH and 6-OH of BA were very low and quite close, however the glucuronidation of the 7-OH in HLM was significantly higher than that of the 6-OH. This is because that the glucuronidation of the flavonoid not only displayed strong regio-selective features, but also displayed isoform specific characteristics.[15] In a study conducted with 7 mono-hydroxyflavone, UGT1A1 and 1A9 showed higher activity towards the 7-OH than 6-OH of seven mono-flavonoids while UGT1A8 and UGT1A10 displayed higher catalytic activity of the 6-OH than 7-OH.[15] UGT1A8 and UGT1A10 are expressed mainly in human intestine, but not in HLM, while UGT1A9 is not expressed in HIM. These results indicated that the BDE of the substrate is an important factor which could determine the glucuronidation activity but the structure of the enzyme also played some role in the metabolic site selection. The calculated BDE matched well with the experimental results and most of the UGT reactions can be interpreted by reaction energy theory. Therefore, this calculated BDE of the substrate can be used as a predictive tool for the study of glucuronidation reactions. However, further calculations and experimental work are required to validate this method. As the calculated BDE is purely from the substrate approach, without considering the enzyme structure and other factors, we realized that it has some limitations.

Conclusion

In the present study, our results demonstrated that structural modifications by introducing a Mannich base substituent at the C-8 position of baicalein could strongly improve the glucuronidation stability. The enhance glucuronidation stability was achieved from the following three aspects including blocking of 7-O-glucuronidation by IMHB, reduction of the involved UGT isoforms and decreasing the inherent clearance of 6-O-glucuronidation. Factors such as the IMHB, molecular volume and the hydrophobicity of substrates can affect the UGT-mediated biotransformation in different ways. These findings bring novel insights into the structure-glucuronidation relationship and provide some new solutions for modulating the glucuronidation stability of drug candidates. Furthermore, this study opens an avenue for using calculation to analyze the potential ability of compound which is metabolized by human UGTs.

Experimental

Reagents and Materials

BA-a (purity>98%) and BA-j (purity>98%) were synthesized by Professor Shixuan Zhang's Lab, Dalian University of Technology. BA (purity > 98%), baicalin (BA 7-O-glucuronide) (purity > 98%) and 4-methylumbelliferone were purchased from the Victory Company (Chengdu, China). Alamethicin, Brij 58, magnesium chloride, D-saccharic acid, 1, 4-lactone, β-glucuronidase and uridine 5'-diphospho-glucuronic acid trisodium salt (UDPGA) were purchased from Sigma-Aldrich (St. Louis, MO, USA). 1, 4-dithio-DL-threitol (DTT) (99%) was purchased from Alfa Aesar (Lancashire, UK). SPE C18 cartridges were purchased from Bonna-Agela Technologies (Wilmington, DE, USA). HLM (Lot. DXOV) pooled from 11 donors, HLS9 (Lot. PBCQ) pooled from

11 donors and RbLM (Lot. PSGA) were purchased from the Research Institute for Liver Diseases (Shanghai, China). A panel of 12 recombinant human UGT isoforms (UGT1A1, 1A3, 1A4, 1A6, 1A7, 1A8, 1A9, 1A10, 2B4, 2B7, 2B15, and 2B17) expressed in baculovirus-infected insect cells were purchased from BD Gentest Corp (Woburn, MA, USA). All other reagents were of HPLC grade or of the highest grade commercially available.

Glucuronidation Assays

BA-a, BA-j and BA at various concentrations were incubated with HLM, RbLM, or recombinant human UGT isoforms in a reaction mixture containing 50 mM Tris-HCl buffer (pH 7.4), 5 mM $MgCl_2$, and 10 mM D-saccharic acid 1,4-lactone, DTT 4mM in a final volume of 200 μL. When HLM or RbLM were assayed, the microsomes were fully activated by the addition of alamethicin (5% protein w/v) or Brij 58 (0.1 mg/mg protein). Reaction mixtures were pre-incubated at 37°C for 5 min and initiated by addition of UDPGA to a final concentration of 4 mM. The samples were incubated for certain periods of time and the reaction terminated by addition of 100 μL ice-cold acetonitrile and then centrifuged at 20,000g, 4°C, for 20 min. Control incubations were performed either without microsomes, without UDPGA or without substrate. The supernatants were subjected to ultra-fast liquid chromatography (UFLC) coupled with a diode array detector (DAD) and electrospray ionization (ESI) mass spectrometer (MS) analyzer.

Analytical Methods

BA, BA-a and BA-j glucuronidation samples were analyzed by a UFLC spectrometry system (Shimadzu, Kyoto, Japan), equipped with two LC-20AD pumps, a DGU-20A3 vacuum degasser, a SIL-20ACHT auto-sampler, a CTO-20AC column oven, an SPD-M 20A DAD, a CBM-20A communications bus module, a mass detector (2010EV) with an ESI interface, and a computer equipped with UFLC-MS solution software (version 3.41; Shimadzu). A Shim-pack VP-ODS (150.0 × 2.0 mm i.d.; 3 μm; Shimadzu) analytical column with an ODS guard column (5 × 2.0 mm i.d.; 2.2 μm; Shimadzu) was used to separate these flavonoids and their glucuronides. The column temperature was kept at 40°C. The mobile phase was acetonitrile (A) and water containing 0.2% formic acid (B) at a flow rate of 0.4 mL/min. For BA analysis, the following gradient was used: 0 to 10 min, 90% B to 55% B, 10 to 13 min, 5% B, 13 to 17 min balance to 90% B. For BA-a and BA-j analysis, the gradient was: 0 to 10 min 90% to 70% B, 10 to 13 min, 5% B, 13 to 17 min balance to 90% B. The glucuronidation samples were quantified by the standard concentration curve of the baicalin, BA-a and BA-j at the detector wavelength of 320 nm. The quantification of BA-a and BA-j glucuronides was calibrated with the ratio of UV absorbance of BA-a and BA-j substrates and their corresponding glucuronides which obtained by hydrolyzing the metabolites with β-glucuronidase. BA, BA-a and BA-j were detected at 320 nm wavelength which were linear from 0.1 to 20 μM, with correlation coefficients R^2 of 0.9952, 0.991and 0.9997 respectively. The quantitative method displayed good sensitivity, with the limit of detection of flavonoids glucuronide close to 0.5 ng. The method also displayed good reproducibility, with the intra-day and inter-day variances both less than 3%.

Mass detection was performed on a Shimadzu LCMS-2010EV instrument with an ESI interface in negative ion mode from *m/z*100 to 800. The detector voltage was set at -1.55 kV for negative ion detection. The curved desolvation line temperature and the block heater temperature were both set at 250°C, whereas the curved desolvation line voltage was set at 40 V. Other MS detection conditions were as follows: interface voltage, 4.5 kV and +4.0 kV for positive and negative ion detection, respectively; nebulizing gas (N_2) flow, 1.5 L/min, and drying gas (N_2) pressure, 0.06 MPa. Data processing was performed using the LC-MS solution software (version 3.41; Shimadzu).

Half-life Assays

To evaluate the glucuronidation stability of BA and its derivatives, $t_{½}$ tests were carried out. BA, BA-a and BA-j 5μM were incubated with 0.5mg/mL of HLS9 respectively in a reaction mixture containing 50 mM Tris-HCl buffer (pH 7.4), 5 mM $MgCl_2$, and 10 mM D-saccharic acid 1,4-lactone, DTT 4mM in a final volume of 200μL. Reaction mixtures were pre-incubated at 37°C for 5 min and initiated by addition of UDPGA to a final concentration of 2 mM and terminated with 100μL ice-cold acetonitrile at 0, 5, 15, 30, 40 min. After sample centrifugation, the supernatants were subjected to UPLC detection. Under first-order kinetics, the rate of metabolism is proportional to the compound concentration, so the rate decreases over time.[45,46] The calculation of $t_{1/2}$ was according to equation (1).

$$t_{1/2} = \frac{\ln 2 \times t}{\ln(c\%)} \quad (1)$$

Where t is the time of incubation, c% is the percentage of the substrate remaining over time.

Biosynthesis of Metabolites and Their Structural Characterization

To identify the glucuronidation site of BA-a and BA-j, a large amount of BA-a glucuronide and BA-j glucuronide were biosynthesized with RbLM and purified for structural elucidation and hydrolysis experiments. Preliminary experiments found that RbLM catalysed the glucuronidation of BA-j and BA-a with high efficiency. In RbLM, BA-a and BA-j glucuronidation produced the same metabolite as it did in HLM. The experimental method was according to Zhu et al. with slight modifications.[47] In brief, 500 μM BA-j or BA-a was incubated with RbLM (0.5 mg/mL) protein which was pre-treated with Brij 58 (0.1 mg/mg protein), 50 mM Tris-HCl (pH 7.4), 5 mM $MgCl_2$, 4mM DTT and 2 mM UDPGA in 70 mL of reaction mixture for 5 hrs at 37°C. The reaction was put on ice to cool it, and then the mixtures were centrifuged at 4 °C for 30 min. The supernatant was loaded on a C18 SPE cartridge to desalt. The SPE cartridge was preconditioned by sequenti...

washing with 6 mL of methanol and 6 mL of deionized water before the sample was loaded on the cartridge. After sample loading, the SPE column was sequentially washed with 6 mL of deionized water and 12 mL of methanol. Finally, 5 mL of methanol containing 5% formic acid was used to elute both the metabolite and its substrate. The entire process was monitored by UFLC-MS, and the metabolite was assembled in methanol containing 5% formic acid. Then the sample was concentrated with a vacuum evaporator to reduce the volume. The sample was separated from its untransformed substrate by preparative liquid chromatography and the fraction of metabolite was collected and dried with a vacuum evaporator at 45°C. The metabolite was dissolved in DMSO-d6 (Euriso-Top, Saint-Aubin, France) for NMR analysis. The structure of the metabolite was determined by NMR spectra including ^{1}H NMR, ^{13}C NMR, heteronuclear singular quantum correlation (HSQC) and heteronuclear multiple bond correlation (HMBC). All experiments were performed on a Bruker 500 MHz NMR Spectrometer. Chemical shifts were reported in parts per million (ppm, δ scale) and referenced to tetramethylsilane at 0 ppm for ^{1}H NMR (500 MHz) and ^{13}C NMR (125 MHz).

Hydrolysis of Glucuronides

To confirm the glucuronides were β-type and to calibrate the metabolite standard curve, M1 of BA-a and metabolites of BA-j were hydrolyzed with β-glucuronidase. In brief, 10 μL of metabolite (dissolved in DMSO) was added in 190 μL Tris-HCl buffer (50 mM, pH7.4). β-glucuronidase 103000 U/μL was diluted with 150 mM sodium acetate buffer (pH 5.0) to 4000 U/μL. The Tris-HCl solution of metabolite and the diluted β-glucuronidase were mixed at 1:1 (v:v). Mixtures without β-glucuronidase were run as controls. The hydrolyzed and control samples were incubated at 37℃ for 90 min, and then the reactions were terminated with 200 μL acetonitrile. After centrifugation, the supernatants were injected for UPLC-DAD analysis. The experiments were run in two independent experiments in duplicate. The UV absorbance ratio between glucuronide and its corresponding aglycon was calculated.

UGT Reaction Phenotyping

BA, BA-a and BA-j (20 μM, 200 μM) were incubated with recombinant human UGT isoforms; the enzyme concentrations were 0.1 mg/mL and the reaction conditions were same as in the glucuronidation assay. The incubation period was 60 min. After reaction, the samples were centrifuged and the supernatants were injected for UPLC-DAD analysis.

Kinetic Analysis

To obtain the kinetic parameters in HLM, BA-a (0-510 μM) was incubated with pooled HLM (0.5 mg/mL), BA-j (0-720 μM) was incubated with pooled HLM (0.05 mg/mL) at 37°C for 60 min. BA (0-500 μM) was incubated with pooled HLM (0.01 mg/mL) at 37°C for 13 min. Kinetic analysis for BA-a and BA-j in UGT1A1 and UGT1A9 were also performed. BA-a (0-510 μM) was incubated with UGT1A1 (0.5 mg/mL)/UGT1A9 (0.6 mg/mL) at 37°C for 60 min. BA-j (0-720 μM) was incubated with UGT1A1 (0.05 mg/mL) or UGT1A9 (0.1 mg/mL) at 37°C for 60 min. Preliminary experiments were performed to guarantee that the formation of the glucuronide was in the linear range with both time and protein concentrations. Due to low concentrations of metabolites being formed, the kinetics of BA-a and BA-j in UGT1A3, 1A8, 2B15 and 2B17 were not performed. The kinetic models employed were either substrate inhibition (eq.2) or Michaelis-Menten (eq.3). For substrate inhibition:

$$v = \frac{V_{\max}[S]}{K_S + [S] + [S]^2 / K_{si}} \quad (2)$$

Where v is the rate of the reaction, [S] is the substrate concentration, V_{max} is the maximum velocity estimate, K_s is the substrate affinity constant, and K_{si} is the substrate inhibition constant.

For the Michaelis-Menten kinetic model:

$$v = \frac{V_{\max} \times [S]}{K_m + [S]} \quad (3)$$

Where v is the rate of reaction, [S] is the substrate concentration, V_{max} is the maximum velocity estimate, and K_m is the apparent affinity constant.

All incubations were performed in duplicate. Kinetic constants were obtained using GraphPad Prism 5 (GraphPad Software, Inc. La Jolla, CA) software.

Computational Method

The hydrogen detached energy (or bond dissociation energy, BDE) of the C-5, C-6 and C-7 phenolic groups in BA, BA-a and BA-j were calculated theoretically using the density function theory. All molecules (including neutral and free radicals) were first energy optimized using the B3LYP method and 6-31+g(d) basis set. Then frequency calculations were performed to validate that all the optimized structures were on the energy minima of potential energy surface (no imaginary frequencies). The BDE is defined as the enthalpy difference between the free radicals (radicals of molecule and hydrogen) and the corresponding neutral molecule. All density functional theory calculations were carried out using Gaussian 09 (Revision C.01) software.

Acknowledgements

We thank Miss Ruth M Shepherd for the English language assistance with this manuscript. This work was supported by the National Science & Technology Major Project of China (2012ZX09501001 & 2012ZX09506001), the International Science & Technology Cooperation Program of China (2012DFG32090), the 973 Program (2013CB531800), and NSF of China (81273590 & 81473181).

References

1 H. Z. Lee, H.W. Leung, M.Y. Lai, C. H. Wu. *Anticancer Res,* 2005, **25**: 959–964.
2 H. Leung, W. H. Yang, M. Y. Lai, H. Z. Lee. *Fd Chem. Toxic.* 2007, **45**: 403-411.
3 M. Li-Weber *Cancer Treat Rev*, 2009, **35**:57-68.
4 Y. Chen, S. Shen, L. Chen, T. Lee, L. Yang. *Biochem Pharmacol*, 2001, **61**: 1417-1427.
5 Y. Shen, W. Chiou, Y. Chou, C. Chen. *Eur J Pharmacol*, 2003, **465**: 171-181.
6 H. Hamada, M. Hiramatsu, R. Edamatsu, A. Mori. *Arch Biochem Biophys,* 1993, **306**, 1: 261-266.
7 D. Shieh, L. Liu, C. Lin. *Anticancer Res,* 2000, **20**, 5A: 2861-2865.
8 K. Zandi, B. T. Teoh, S. S. Sam, P. F. Wong, M. R. Mustafa, S. Abubaker. *BMC Complement Altern Med.* 2012, **12**, 1–9.
9 J. Johari, A. Kianmehr, M. R Mustafa, S. Abubakar, K. Zandi. *Int J Mol Sci,* 2012, **13**:16785-16795.
10 L. Zhang, G. Lin, Q. Chang, Z. Zuo. *Pharm Res,* 2005, **22**: 1050-1058.
11 L. Zhang, G. Lin, Z. Zuo. *Pharm Res,* 2007, **24**:81-89.
12 L. Yang, X. Guo, Q. Wang, Y. Chen, Y. Che, Q. Che. *Journal of Chinese Pharmaceutical Sciences,* 2011, **20**:275-281.
13 L. Zhang, C. Li, G. Lin, P. Krajcsi and Z. Zuo. *The AAPS Journal*, 2011, **13**: 378-389.
14 J. Williams, R. Hyland, B. Jones, D. Smith, S. Hurst, T. Goosen, V. Peterkin, J. Koup, S. Ball. *Drug Metab Dispos*, 2004, **32**, 1201-1208.
15 L. Tang, L. Ye, R. Singh, B. Wu, C. Lu, J. Zhao, Z. Liu, M. Hu. *Mol Pharm,* 2010, **7**(3): 664–679.
16 L. Zhang, G. Lin, Z. Zuo. *Life Sciences.* 2006, **78**: 2772 – 2780.
17 R. Singh. PhD dissertation, The University of Houston College of Pharmacy. 2010. **http://hdl.handle.net/10657/ETD-UH-2010-05-33.**
18 Z. Liu and M. Hu. *Expert Opin Drug Metab Toxicol.* 2007, **3**(3): 389–406.
19 W. H. Huang, A. R. Lee, P. Y. Chien and T. C. Chou. *J Pharm Pharmacol,* 2005, **57**(2):219-25.
20 S. Huanga, Y. Lee, E. A. Gullena, and Y. Chenga. *Bioorg Med Chem Lett,* 2008, **18**: 5046–5049.
21 A. Rowland, J. O. Miners, P. I. Mackenzie. *Int J Biochem Cell Biol,* 2013, **45**(6):1121–1132.
22 C. Guillemette. *The Pharmacogenomics J,* 2003, **3**, 136-158.
23 X. Chen, H. Wang, Y. Du, D. Zhong. *J Chromatogr B,* 2002, **775**: 169–178.
24 S. Zhang, J. Ma, Y. Bao, P. Yang, L. Zou, K. Li , X. Sun. *Bioorgan Med Chem,* 2008, **16** :7127–7132.
25 S. Zhang, Y.Bao, Y. Sun, K. Li, L. Zou, J. Ma, X. Sun, H. Shang, J. Li. U.S. patent 2013, **8**, 377, 895 B2.
26 M. Natsume, N. Osakabe, M. Oyama, M. Sasaki, S. Baba, Y. Nakamura, T. Osawa, J. Terao. *Free Radic Biol Med,* 2003, **34**:840–849.
27 D. Bowles, E. K. Lim, B. Poppenberger, F. E.Vaistij. *Annu Rev Plant Biol*, 2006, **57**:567-597.
28 H. Yin, G. Bennett, J. P. Jones. *Chem-Biol Interact,* 1994, **90**: 47-58.
29 M. J. Miley, A. K. Zielinska, J. E. Keenan, S. M. Bratton, A. Radominska-Pandya, M. R. Redinbo. *J Mol Biol*, 2007, **369**:498-511.
30 S. Ohno, S. Nakajin. *Drug Metab Dispos*, 2009, **37**:32-40.
31 B. T. Ethell, S. Ekins, J. Wangand B. Burchell. *Drug Metab Dispos*, 2002, **30**:734–738.
32 P. I. Mackenzie, I. S. Owens, B. Burchell, K. W. Bock, A. Bairoch, A. Belanger, S. Fournel-Gigleux, M. Green, D. W. Hum, T. Iyanagi, D. Lancet, P. Louisot, J. Magdalou, J. R. Chowdhury, J. K. Ritter, H. Schachter, T. R.Tephly, K. F. Tipton, D. W. Nebert. *Pharmacogenetics,* 1997, **7**, 255–269.
33 Y. Xia, G. Ge, P. Wang, S. Liang, Y. He, J. Ning, X. Qian, Y. Li, and L. Yang. *Drug Metab Dispos.* 2015, **43**:553–560.
34 S. Krishnaswamy, S. Duan, L. Moltke, D. J. Greenblatt, M. H. Court. *Drug Metab Dispos,* 2003, **31**:133–139.
35 H. Liu, Y. Liu, J. Zhang, W. Li, H. Liu, and L. Yang. *Drug Metab Dispos*, 2008, **36**:1562–1569.
36 M. J. Sorich, P. A. Smith, R. A. McKinnon, J. O. Miners. *Pharmacogenetics,* 2002, **12**:635–645.
37 M. J. Sorich, P. A. Smith, J. O. Miners, P. I. Mackenzie, R. A. McKinnon. *Curr Drug Metab,* 2008, **9**:60–69.
38 B. Wu, J. K. Morrow, R. Singh, S. Zhang, M. Hu. *JPET.* 2011, **336**:403–413.
39 B. Wu, X. Wang, S. Zhang, M. Hu. *Pharm Res.* 2012, **29**:1544-1561.
40 M. F. Hegazi, R. T.Borchardt, R. L.Schowen. *J. Am. Chem. Soc.* 1976, **98**(10) 3048-3049.
41 Y. Kakuta, L. G. Pedersen, C. W. Carter, M. Neqishi, L. C. Pedersen. *Nat Struct Biol*. 1997, **4**(11) 904-908.
42 L.Iyer, C. D. King, P. F.Whitington, M. D. Green, S. K. Roy, T. R.Tephly. *J Clin Invest,* 1998, **101**: 847–854.
43 H. Rosing, V. M. M.Herben, D. M. van Gortel-van Zomeren, E. Hop, J. J. Kettenes van den Bosch, W. W. ten Bokkel Huinink, J. H. Beijnen. *Cancer Chemother Pharmacol,* 1997, **39**:498-504.
44 P. Wang, Y. Xia, Y. Yu, J. Lu, L. Zou, L. Feng, G. Ge, L. Yang. RSC Adv., 2015, **5**, 53477-53483.
45 L. Di, E. H. Kerns, Y. Hong, H. Chen. *Int. J. Pharm.* 2005, **297** (1–2), 110–119.
46 G. Ge, C. Ai, W. Hu, J. Hou, L. Zhu, G. He, Z. Fang, S. Liang, F. Wang, L. Yang. *Eur. J. Pharm. Sciences.* 2013, **48**: 360–369.
47 L. Zhu, G. Ge, H. Zhang, H. Liu, G. He, S. Liang, Y. Zhang, Z. Fang, P. Dong, M. Finel, L. Yang. *Drug Metab Dispos,* 2012, **40**:529–538.